Acid−Base Chemistry of the Reaction of Aromatic L-Amino Acid Decarboxylase and Dopa Analyzed by Transient and Steady-State Kinetics: Preferential Binding of the Substrate with Its Amino Group Unprotonated†

Hideyuki Hayashi, Fuyo Tsukiyama, Seiji Ishii, Hiroyuki Mizuguchi, and Hiroyuki Kagamiyama*

Department of Biochemistry, Osaka Medical College, 2-7 Daigakumachi, Takatsuki 569-8686, Japan

Received April 29, 1999; Revised Manuscript Received July 20, 1999

ABSTRACT: Transient and steady-state kinetic analysis of the reaction of aromatic L-amino acid decarboxylase (AADC), a pyridoxal 5′-phosphate- (PLP-) dependent enzyme, with its substrate dopa was carried out at various pH. The association of AADC and dopa to form the Michaelis complex and the subsequent transaldimination reaction to form the dopa-PLP Schiff base (external aldimine) were followed with a stopped-flow spectrophotometer. Combined with the steady-state k_{cat} value, we could present a minimum mechanism for the reaction of AADC and dopa. In the mechanism, the association of the aldimine-protonated form of the enzyme (EH^+) and the α-amino-group-unprotonated form of the substrate (S) is the main route leading to the Michaelis complex. In addition, the association of EH^+ and the α-amino-group-protonated form of the substrate (SH^+) to form a Michaelis complex $EH^+{\cdot}SH^+$ was also found as a minor route. The pK_a of the α-amino group of dopa was expected to be decreased in the Michaelis complex, promoting the conversion of $EH^+{\cdot}SH^+$ to $EH^+{\cdot}S$, the species that directly undergoes transaldimination to form the external aldimine complex. The association of EH^+ and S had been identified as a minor route for the reaction of aspartate and aspartate aminotransferase (AspAT), which has an unusually low pK_a value of the aldimine and can use the aldimine-unprotonated form (E) of the enzyme for adsorbing the prevalent species SH^+ [Hayashi and Kagamiyama (1997) *Biochemistry 36*, 13558−13569]. The present study implies that, in most PLP enzymes that have a high pK_a value of the aldimine like AADC, S preferentially binds to the enzyme (EH^+). The minor route of $EH^+ + SH^+$ in AADC may be related to the flexibility of the protein in the Michaelis complex, and a simulation analysis showed that the presence of this route decreases the k_{cat} value while increasing the k_{cat}/K_m value. It also suggested that AADC has evolved to suppress the minor route to the extent necessary to obtain the maximal k_{cat} value at neutral pH.

In the catalytic process of pyridoxal 5′-phosphate- (PLP-)[1] dependent enzymes, the substrate amino acid forms a Schiff base (aldimine) with PLP, and the electrophilicity of the PLP pyridine ring plays important roles in the subsequent catalytic steps. Because PLP forms an aldimine with the ϵ-amino group of a lysine residue at the active site of the unliganded enzyme, a transaldimination reaction between the PLP-Lys aldimine and the substrate α-amino group occurs. This reaction has been extensively studied for aspartate aminotransferase (AspAT; refs *1*−*5*). In AspAT, the PLP-Lys258 aldimine has an unusually low pK_a of 6.8 and is largely unprotonated at neutral pH. The aldimine-unprotonated form of the enzyme (E) accepts the α-amino-group-protonated form (SH^+)[2] of the substrate aspartate to form a Michaelis complex ($E{\cdot}SH^+$). The proton on the ammonium group of the substrate is transferred onto the imine group of the aldimine, the basicity of which is increased through the enzyme−substrate interaction, to form the second Michaelis complex ($EH^+{\cdot}S$). This complex, with the lone-pair electrons on the substrate amino group unmasked and the electrophilicity of the imine group increased by protonation, is the species that directly undergoes transaldimination. This route, first presented by Karpeisky and Ivanov (*6*), accounted for the significance of the low pK_a value of the PLP aldimine of AspAT in accepting the amino-group-protonated form of aspartate, the prevalent form at neutral pH. However, most PLP enzymes have high pK_a values of the aldimine, generally over 10, as judged from the spectroscopic measurements (*7*). Therefore, the Karpeisky−Ivanov mechanism of AspAT cannot be directly applied to the other PLP enzymes. Recently, we showed the presence of a second route for the association of aspartate and AspAT (*4*), that is, the association of the aldimine-protonated form of the enzyme (EH^+)

† This work was supported by research grants from the Japan Society for the Promotion of Science ("Research for the Future" Program 96L00506 and Grant-in-Aid for Scientific Research 00183913) and a SUNBOR Grant from the Suntory Institute for Bioorganic Research.

* To whom correspondence should be addressed: Telephone +81-726-84-6416; Fax +81-726-82-6851; e-mail med001@art.osaka-med.ac.jp.

[1] Abbreviations; AADC, aromatic L-amino acid decarboxylase (aromatic L-amino acid carboxy-lyase, EC 4.1.1.28); AspAT, aspartate aminotransferase (aspartate:2-oxoglutarate aminotransferase, EC 2.6.1.1); EDTA, ethylenediaminetetraacetic acid; K-P_i, potassium phosphate buffer; MES, 4-morpholineethanesulfonic acid; PIPES, 1,4-piperazinebis(ethanesulfonic acid); TAPS, 3-[[tris(hydroxymethyl)methyl]-amino]-1-propanesulfonic acid.

[2] The amino group is protonated and the two carboxyl groups are deprotonated.

10.1021/bi9909795 CCC: $18.00
Published on Web 11/05/1999

and the α-amino-group-unprotonated form of the substrate (S) to form directly the Michaelis complex EH^+•S. Although this route has an auxiliary significance in the reaction mechanism of AspAT, it was highly expected that in many PLP enzymes, which have a high pK_a value of the aldimine, this route may be the main pathway of the catalytic reaction. Alternatively, we can consider a scheme in which the amino-group-protonated substrate binds to the enzyme and, after deprotonation of the amino group, undergoes transaldimination. To examine which mechanism works for PLP enzymes in general, we set out to investigate the reaction of aromatic L-amino acid decarboxylase (AADC) with its substrate 3,4-dihydroxyphenylalanine (dopa). The advantage of using AADC for this study is that it is one of the enzymes for which the enzyme−substrate association process can be followed spectroscopically (*9*).

EXPERIMENTAL PROCEDURES

Enzyme. Rat liver AADC was expressed in *Escherichia coli* MD55 (*8*) transformed with pKKAADCII (*9*). The purification procedure was modified from the previous one (*9*) as follows. All the procedures were carried out at 0−4 °C. Buffers contained 0.1 mM dithiothreitol, 0.1 mM EDTA, and 5 μM PLP as stabilizing agents. Thirty grams of *E. coli* cells was suspended in 70 mL of 20 mM potassium phosphate buffer (K-P_i), pH 7.0, and the cells were disrupted at 0 °C for 10 min with a Branson Sonifier model 350 set at output 6 and 50% duty. Cell debris was removed by centrifugation (10000*g*, 40 min). Solid ammonium sulfate was added to 25% saturation while the pH was maintained at 7.0 with 1 M KH_2PO_4. Insoluble proteins were removed by centrifugation (10000*g*, 10 min), and the supernatant was applied to a Phenyl-Sepharose CL-4B column (2.5 × 25 cm) equilibrated with 20 mM K-P_i, pH 7.0, containing 25% saturated ammonium sulfate. The proteins were eluted with a linear gradient formed with 500 g of 20 mM K-P_i, pH 7.0, containing 25% saturated ammonium sulfate, and 500 g of 1 mM K-P_i, pH 7.0. After the gradient was over, the elution was continued with 1 mM K-P_i, pH 7.0. After about 80 mL elution of the 1 mM buffer, fractions with intense brown color emerged and lasted for about 40 mL. These fractions contained high AADC activity. The fractions were combined, concentrated to ∼10 mL, dialyzed against 500 mL of 5 mM K-P_i, pH 7.0, for 3 h, and applied to a DEAE-Toyopearl 650M column (2.5 × 25 cm) equilibrated with 5 mM K-P_i, pH 7.0. The column was washed with 100 mL of the 5 mM buffer, and the proteins were eluted with a 1-L linear gradient of 0−0.1 M NaCl in 5 mM K-P_i, pH 7.0. The first protein peak, which emerged at around 300 mL elution, contained mainly AADC. The high-purity fractions were combined, concentrated to about 10 mL, and applied to a hydroxyapatite column (2.5 × 25 cm) equilibrated with 5 mM K-P_i, pH 7.0. AADC was eluted with a 1-L linear gradient formed with 5 and 100 mM K-P_i, pH 7.0. AADC was eluted at about 500 mL elution. The final preparation (∼50 mg) was essentially homogeneous as judged from sodium dodecyl sulfate−polyacrylamide gel electrophoresis (data not shown). This simplified purification procedure requires no desalting of the enzyme solution for the next step, and the entire purification can be done within 3 days.

Chemicals. L-3,4-Dihydroxyphenylalanine (dopa) was obtained from Nakarai Chemicals (Kyoto, Japan). L-Dopa methyl ester was from Sigma. All other chemicals were the highest grade commercially available.

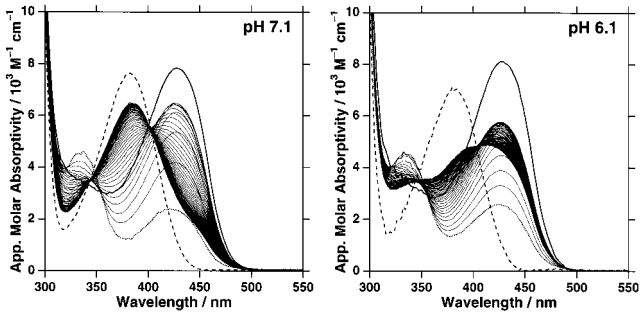

FIGURE 1: (Left) Time-resolved spectra for the reaction of AADC and dopa at pH 7.1. Enzyme (30 μM) and dopa (0.5 mM) were reacted in 50 mM PIPES−NaOH, pH 7.1 at 298 K. Bold dotted line represents the spectrum of AADC in the absence of dopa. After the addition of dopa, spectra were taken between 1.28 and 49.92 ms at 2.56-ms intervals. (Right) Same as the left except that the reaction was carried out in 50 mM PIPES−NaOH, pH 6.1. In each panel, the bold line and the bold dashed line represent the spectrum of the Michaelis complex and the external aldimine complex calculated from the time-resolved spectra (see text).

Spectroscopic Analysis. Absorption spectra were measured on a Hitachi U-3300 spectrophotometer at 298 K. The buffer solution contained 50 mM buffer component(s) and 0.1 mM EDTA. The buffer components used were MES−NaOH, HEPES−NaOH, and TAPS−NaOH. Enzyme (subunit) concentrations were generally (1−3) × 10^{-5} M, which were determined spectrophotometrically. The apparent molar extinction coefficient at 280 nm was $\epsilon_M = 7.9 \times 10^4$ M^{-1} cm^{-1} (*9*).

Kinetic Analysis. Stopped-flow spectrophotometry was performed on an Applied Photophysics (Leatherhead, U.K.) SX.17MV system at 298 K. The dead time was generally 2.3 ms under a gas pressure of 500 kPa. The exponential absorption changes were analyzed by using the program provided with the instrument. Time-resolved spectra were collected on the SX.17MV system equipped with a photodiode array accessory and the XScan (version 1.0) control software.

For steady-state kinetics, enzyme activity was measured by the fluorometric method (*8*), in which the product dopamine is separated from dopa with a cation-exchange resin column, derivatized into a fluorescent compound through oxidative conjugation with ethylenediamine, and then quantified. The catalytic reactions were carried out in 1 mL of 50 mM buffer solution containing 0.1 mM EDTA, 5 μM PLP, and various concentrations of dopa. PLP was added simultaneously with the enzyme, to minimize the Pictet−Spengler reaction between dopa and PLP (*10*).

RESULTS

Transition of the Spectrum of AADC upon Reaction with Dopa. AADC has a large absorption band at 335 nm and a smaller one at 425 nm, irrespective of the solution pH (*9*). When AADC was reacted with dopa, a rapid increase in the 425 nm absorbance and a concomitant decrease in the 335 nm absorbance were initially observed. This was followed by a slow decrease in intensity of the two absorption bands and concomitant emergence of a new absorption band at 380 nm (Figure 1). The emergence of the 380-nm absorption band was more apparent at higher pH (Figure 1). This can be

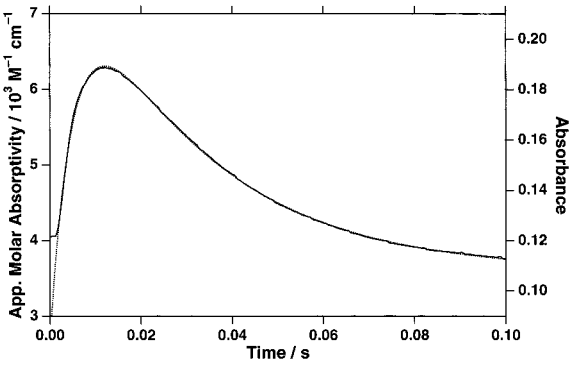

FIGURE 2: Time course of the absorption change during the reaction of AADC and dopa. Enzyme (30 μM) was mixed with 0.4 mM dopa in 50 mM PIPES, pH 7.0, and the absorbance at 420 nm was monitored. The flow was stopped at 2.0 ms. Curve-fitting (dotted line) was performed by use of eq 1 within the region between t = 2.0 and 100 ms. The values of the parameters obtained after the fitting procedure were $A_{fast} = -0.176 \pm 0.0005$, $k_{fast} = 192 \pm 1$ s^{-1}, $A_{slow} = 0.149 \pm 0.0005$, $k_{slow} = 33.8 \pm 0.1$ s^{-1}, and $A_{SS} = 0.108 \pm 0.0001$.

attributed to the pH-dependent change in the equilibrium between the external aldimine complex and the two structures of the Michaelis complex (see Absorption Spectra of the Reaction Intermediates). After the slow phase was over, the absorption spectrum did not change, reflecting that the reaction reached steady state. The biphasic change in the absorbance could be fit to a biexponential equation (Figure 2):

$$A = A_{fast}e^{-k_{fast}} + A_{slow}e^{-k_{slow}} + A_{SS} \quad (1)$$

where the first and second terms represent the absorption change in the fast phase and the slow phase, respectively, and A_{SS} is the absorbance at steady state. The values of k_{fast} and k_{slow} were independent of the wavelength between 300 and 550 nm, as reflected by the presence of an isosbestic point in the fast phase and two isosbestic points in the slow phase. The reaction was followed at pH values between 5.9 and 8.2, and the k_{fast} and k_{slow} values were obtained at each pH. The pH dependency of the values was analyzed as follows.

pH Dependency of k_{+1} and k_{-1}. The biexponential transition of the spectra can be analyzed on the basis of the two-step mechanism (*9*):

$$EH^+ + S^\circ \underset{k_{-1}}{\overset{k_{+1}}{\rightleftharpoons}} ES_1 \underset{k_{-2}}{\overset{k_{+2}}{\rightleftharpoons}} ES_2 \xrightarrow{k_{+3}} EH^+ + P \quad (2)$$

where EH^+, S°, ES_1, ES_2, and P represent the unliganded enzyme, the free substrate, the Michaelis complex, the external aldimine complex, and the product, respectively. The symbols EH^+ and S° have been modified from the previous ones. EH^+ indicates that the aldimine of AADC is always protonated. S° includes both S and SH^+, because at present we have no information about the protonation state of the substrate that reacts with AADC. The k_{fast} and k_{slow} values are related to the individual rate constants as follows (*9*):

$$k_{fast} = k_{+1}[S^\circ] + k_{-1} \quad (3)$$

$$k_{slow} = k_{+2} + k_{-2} + k_{+3} \quad (4)$$

The [S°] and pH dependency of the k_{fast} value is shown in Figure 3A. At each pH, the k_{fast} value showed a linear

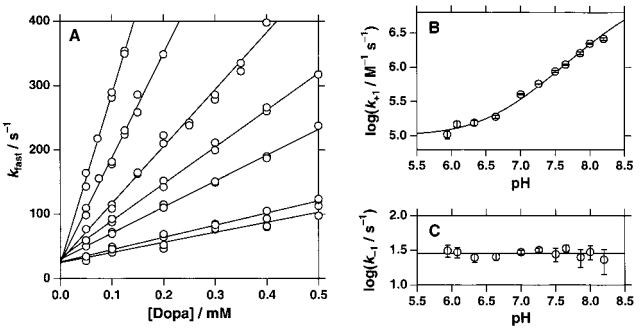

FIGURE 3: (A) Dependency on the dopa concentration and pH of the apparent rate constant for the fast phase of the spectral change (k_{fast}). The k_{fast} values were obtained by fitting the absorption change at 430 nm to eq 1. The pH values of the solution are, with increasing slope of the plots, 6.1, 6.6 7.0, 7.3, 7.7, 7.9, and 8.2. (B) Plots of log k_{+1} determined from the slope of the plots in panel A against pH. (C) Plots of log k_{-1} determined from the intercepts at the abscissa in panel A against pH. In panels B and C, bars represent SD.

dependency on [S°], which conformed well to eq 3. The k_{+1} and k_{-1} values were obtained from the slope and the intercept on the ordinate, respectively. Apparently, the value of k_{+1} was increased with increasing pH, that is, the association of dopa and AADC became faster by increasing the fraction of the species of dopa with unprotonated α-amino group (S). If only S binds to the enzyme and SH^+ does not, we should obtain a slope of 1 for the plot of log k_{+1} in the pH region sufficiently lower than 8.7, the pK_a value of the α-amino group of dopa (*11*). However, as shown in Figure 3B, the slope was smaller than unity. This indicated that SH^+ can also, although more weakly, bind to the enzyme. The association of dopa and AADC should then be analyzed on the basis of the following scheme:

$$\begin{array}{ccccccc} EH^+ + S & \underset{k^S_{-1}}{\overset{k^S_{+1}}{\rightleftharpoons}} & EH^+\cdot S & \underset{k_{-2}}{\overset{k^{int}_{+2}}{\rightleftharpoons}} & ES_2 & \xrightarrow{k_{+3}} & EH^+ + P \\ K_a^\alpha \updownarrow & & \updownarrow K_a^{\alpha M} & & & & \\ EH^+ + SH^+ & \underset{k^{SH}_{-1}}{\overset{k^{SH}_{+1}}{\rightleftharpoons}} & EH^+\cdot SH^+ & & & & \end{array} \quad (5)$$

where K_a^α and $K_a^{\alpha M}$ indicate the proton dissociation constant for the α-amino group of dopa and that in the Michaelis complex. The superscript int of k^{int}_{+2} indicates that the rate constant is the intrinsic one for the transaldimination reaction from $EH^+\cdot S$ to ES_2. The k_{+1} and k_{-1} values obtained from the slope and the intercept on the ordinate, respectively, of Figure 3A are expressed as:

$$k_{+1} = \frac{10^{-pK_a^\alpha}}{10^{-pH} + 10^{-pK_a^\alpha}}(k^S_{+1}) + \frac{10^{-pH}}{10^{-pH} + 10^{-pK_a^\alpha}}(k^{SH}_{+1}) \quad (6)$$

$$k_{-1} = \frac{10^{-pK_a^{\alpha M}}}{10^{-pH} + 10^{-pK_a^{\alpha M}}}(k^S_{-1}) + \frac{10^{-pH}}{10^{-pH} + 10^{-pK_a^{\alpha M}}}(k^{SH}_{-1}) \quad (7)$$

The pK_a^α value is known to be 8.7. Fitting of eq 6 to the data yielded $k^S_{+1} = (1.3 \pm 0.06) \times 10^7$ M^{-1} s^{-1} and $k^{SH}_{+1} = (1.0 \pm 0.08) \times 10^5$ M^{-1} s^{-1}. As shown in Figure 3A, the value of the intercept on the ordinate was around 28 s^{-1} and was essentially independent of the solution pH between 5.9 and 8.2 (Figure 3C). The simplest interpretation of this

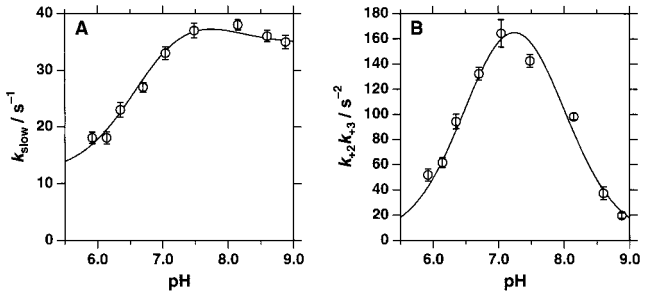

FIGURE 4: (A) Plots of k_{slow} ($= k_{+2} + k_{-2} + k_{+3}$) versus pH of the solution. (B) Plots of $k_{+2}k_{+3}$ versus pH of the solution. The value of $k_{+2}k_{+3}$ at each pH was calculated from the value of k_{slow} obtained from the transient kinetics and k_{cat} from the steady-state kinetics using eq 8. In each panel, the solid line is the theoretical curve derived from eqs 10 and 11 (see text). Fitting was performed simultaneously for k_{slow} and $k_{+2}k_{+3}$. Bars represent SD.

observation is that both k^{S}_{-1} and k^{SH}_{-1} have the same value of $28 \pm 1\ s^{-1}$. The $pK^{\alpha M}_{a}$ value is then determined to be 6.6 ± 0.07 from the thermodynamic cycle of eq 5. Another possibility is that k^{SH}_{-1} is much higher than k^{S}_{-1} and $pK^{\alpha M}_{a}$ is sufficiently lower than 5.9 so that k_{-1} has an almost constant value above pH 5.9. If this is the case, the Michaelis complex exists predominantly as the form of $EH^{+}\cdot S$. Accordingly, the spectrum at steady state in the presence of a sufficient concentration of dopa, which is a mixture of the spectra of the Michaelis complex and the external aldimine, should be constant irrespective of pH. That the spectrum at steady state has a smaller absorption band at 380 nm at lower pH (Figure 1) excludes the second mechanism described immediately above.

pH Dependency of k_{+2}, k_{-2}, and k_{+3}. Transient kinetics of a pre-steady-state reaction alone cannot determine all of the kinetic parameters and requires combination with steady-state kinetics. We determined the kinetic parameters other than k_{+1} and k_{-1} as follows.

The transient kinetic analysis could determine the value of $k_{+2} + k_{-2} + k_{+3}$ ($= k_{slow}$). The pH dependency of the value is shown in Figure 4A. On the other hand, the steady-state kinetics gave the values of k_{cat} and K_m, which are related to the parameters of eq 2 by the following equations (*9*):

$$k_{cat} = \frac{k_{+2}k_{+3}}{k_{+2} + k_{-2} + k_{+3}} \tag{8}$$

$$K_m = \frac{k_{-1}k_{-2} + k_{-1}k_{+3} + k_{+2}k_{+3}}{k_{+1}(k_{+2} + k_{-2} + k_{+3})} \tag{9}$$

As dopa undergoes a nonenzymatic condensation reaction with PLP (Pictet−Spengler reaction; *10*), the concentration of dopa in the assay solution is difficult to control. Therefore, the K_m values could not be obtained with high accuracy and were not used for the subsequent analysis. On the contrary, the k_{cat} value could be obtained precisely from the zero-order catalytic reaction in the presence of a high concentration of dopa. The value of $k_{+2}k_{+3}$ was obtained by using eqs 4 and 8 at each pH. The $k_{+2}k_{+3}$ value showed a bell-shaped dependency on pH (Figure 4B). From eq 5, the pH dependency of the k_{+2} value is expressed as

$$k_{+2} = \frac{10^{-6.6}}{10^{-6.6} + 10^{-pH}}(k^{int}_{+2}) \tag{10}$$

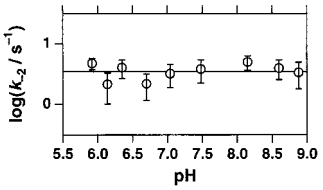

FIGURE 5: Plots of k_{-2} versus pH of the solution. The k_{-2} value was calculated from the value of k_{slow} ($= k_{+2} + k_{-2} + k_{+3}$) and the values of k_{+2} and k_{+3} obtained from Figure 4. Bars represent SD.

Equation 10 can explain the decrease in the $k_{+2}k_{+3}$ value with decreasing pH in the acidic region. However, the decrease in the $k_{+2}k_{+3}$ value with increasing pH in the alkaline region cannot be explained by eq 10. This must be ascribed to the pH-dependent change in k_{+3}.

It is now known that dopa with its α-amino group unprotonated reacts with AADC to form the external aldimine. This indicates that even if the product dopamine goes out of AADC with its α-amino group unprotonated, a proton that is used for protonation of the quinonoid intermediate must enter the active site somewhere in the catalytic cycle. As both k_{+1} and k_{+2} increases with increasing pH (see above), it is reasonable to consider that the entrance of the proton to the active site occurs after the decarboxylation step. Therefore, k_{+3} can be expressed as follows:

$$k_{+3} = \frac{k_{DC}k_{H}[H^{+}]}{k_{DC} + k_{H}[H^{+}]} \tag{11}$$

Here k_{DC} and k_{H} are the rate constants for the decarboxylation and the entrance of the proton to the active site, respectively, and the transaldimination to release the product amine from the aldimine is assumed to be fast compared to the steps of k_{DC} and k_{H}. Simultaneous fitting of the theoretical lines derived from eqs 10 and 11 to the data of k_{slow} ($= k_{+2} + k_{-2} + k_{+3}$) and $k_{+2}k_{+3}$ (Figure 4) yielded the following values: $k^{int}_{+2} = 31 \pm 4\ s^{-1}$, $k_{DC} = 8.0 \pm 1.0\ s^{-1}$, $k_{H} = (6.2 \pm 1.0) \times 10^{8}\ M^{-1}\ s^{-1}$, and $k_{-2} = 3.5 \pm 0.3\ s^{-1}$. During the fitting, we assumed that k_{-2} is independent of pH. If we consider that k_{-2} is dependent on pH, it should be expressed as follows:

$$k_{-2} = (k^{lim,acid}_{-2}\ 10^{-pH} + k^{lim,alkali}_{-2}\ 10^{-pK^{app}_{a}})/(10^{-pH} + 10^{-pK^{app}_{a}}) \tag{12}$$

where $k^{lim,acid}_{-2}$ and $k^{lim,alkali}_{-2}$ are the acidic and alkaline limiting values of k_{-2}. However, for any fixed pK^{app}_{a} values (every 0.25 between 6.0 and 9.0), fitting to the data of k_{slow} ($= k_{+2} + k_{-2} + k_{+3}$) and $k_{+2}k_{+3}$ resulted in almost identical values of $k^{lim,acid}_{-2}$ and $k^{lim,alkali}_{-2}$ (around $3.5\ s^{-1}$), indicating that it is not necessary to consider that k_{-2} is dependent on pH. Consistent with this, the k_{-2} value calculated from eqs 10 and 11 and the values of k^{int}_{+2}, k_{DC}, and k_{H}, determined as above, was essentially independent of the solution pH (Figure 5). Because k_{-2} is the rate constant for the reverse transaldimination from the external aldimine complex to the Michaelis complex, this suggests that the external aldimine has only one protonation structure or is composed of structures that have the same number of protons.

The above results conform to the reaction mechanism shown in Scheme 1, in which the microscopic kinetic

Scheme 1: Proposed Mechanism for the Reaction of AADC with Dopa[a]

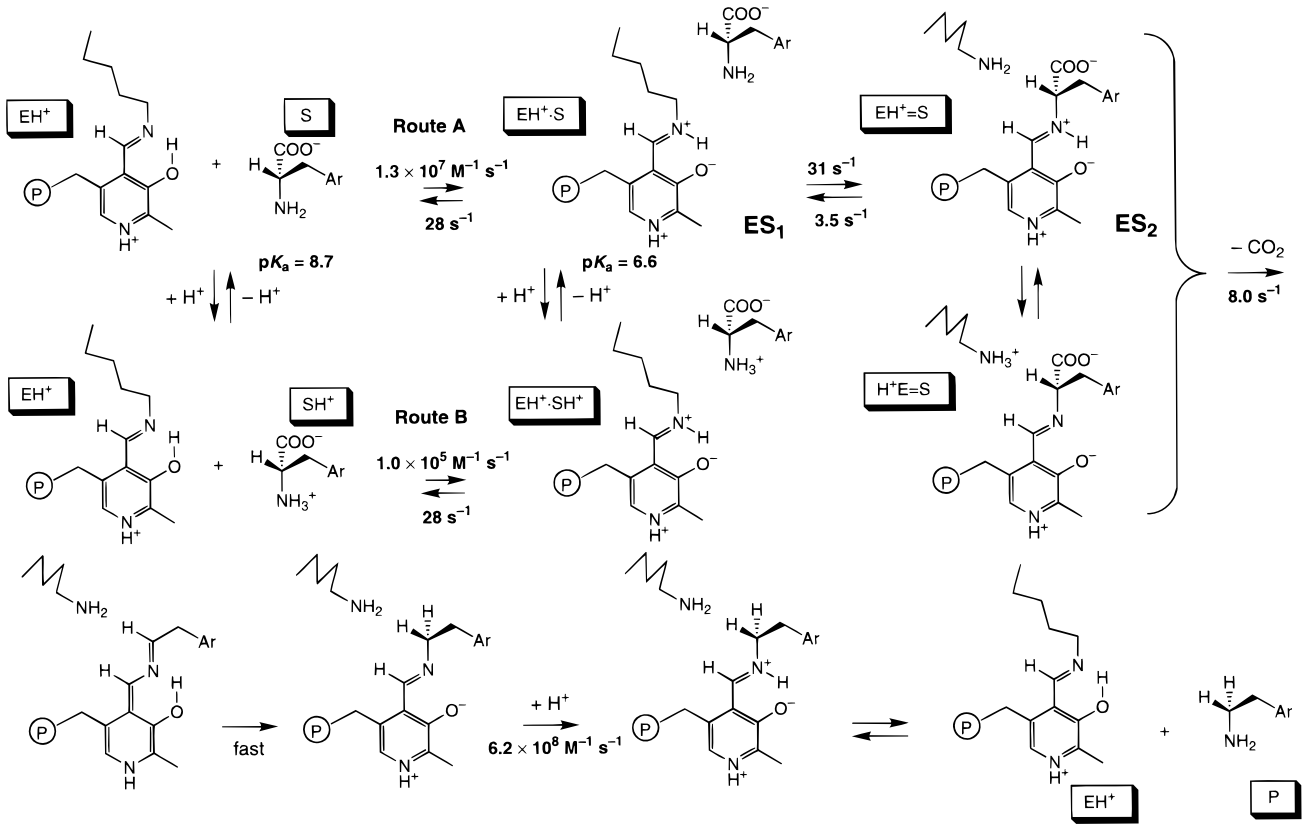

[a] The kinetic parameters determined in this study are shown. The pyridine nitrogen of PLP is considered to be protonated, because AADC has an aspartic acid residue (Asp271) corresponding to Asp316 of ornithine decarboxylase (*18*), which is known to interact with the pyridine N and is proposed to stabilize the positive charge of the protonated pyridine N (*19*). Proton transfer within the quinonoid intermediate and protonation of the unprotonated external aldimine of PLP-dopamine are still hypothetical, although this can explain the experimental results of this study (see Discussion).

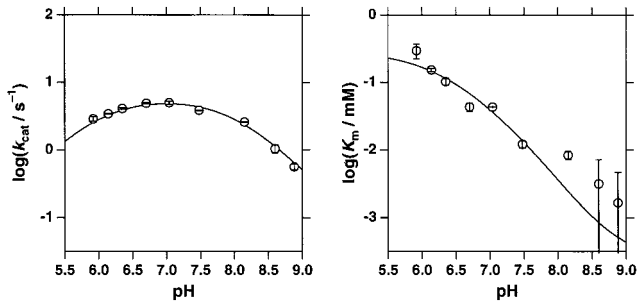

FIGURE 6: Comparison of the steady-state kinetic parameters k_{cat} and K_m obtained experimentally (○) and those calculated from the microscopic parameters and eqs 8−11. Bars represent SD.

parameters are also shown (for the protonation of the quinonoid intermediate, see Discussion).

Validity of the Kinetic Parameters. The microscopic kinetic parameters determined as above were used to simulate the pH dependency of the steady-state kinetic parameters (Figure 6). The value of k_{cat} calculated from eq 8 showed excellent fitting to the experimental values. This can be anticipated, because the experimental k_{cat} values and eq 8 were used to obtain the microscopic kinetic parameters (see above). However, it should be noted that the K_m value calculated from eq 9 also showed good fitting to the experimental values, which had not been used for obtaining the microscopic parameters. Deviation of the experimental K_m values from the theoretical values was observed at higher pH. In this pH region, the Pictet−Spengler reaction between dopa and PLP readily occurs, and the concentration of free dopa is expected to be lower than that calculated from the amount of dopa added to the assay solution. This can be the cause of the apparent large K_m values obtained experimentally at higher pH.

Absorption Spectra of the Reaction Intermediates. Extrapolation to $t = \infty$ of the spectral change during the fast phase yields the apparent spectrum of the equilibrium mixture of EH^+ and ES_1. The absorbance value of the mixture, designated as $A_{lim,fast}$, is expressed as follows:

$$A_{lim,fast} = \frac{k_{-1}}{k_{+1}[S] + k_{-1}}(A_{EH^+}) + \frac{k_{+1}[S]}{k_{+1}[S] + k_{-1}}(A_{ES_1}) \quad (13)$$

where A_{EH^+} and A_{ES_1} are the absorbance values of the free enzyme and the Michaelis complex, respectively. The absorption spectra of the Michaelis complex could be calculated from eq 13, A_{EH^+}, and the microscopic kinetic parameters. The spectra of the external aldimine were obtained from the kinetic parameters and the spectra of the Michaelis complex and those at steady state, from

$$A_{ES_2} = \frac{(k_{+2} + k_{-2} + k_{+3})A_{SS} - (k_{-2} + k_{+3})A_{lim,fast}}{k_{+2}} \quad (14)$$

where A_{ES_2} and A_{SS} are the absorbance values of the external aldimine[3] and the apparent absorbance value of the enzyme at steady state, respectively. The results are summarized in Figure 1. The Michaelis complex showed a large absorption band at 430 nm, reflecting the conversion from the enolimine

form of the Schiff base to the ketoenamine form (*9*; for a detailed discussion of the two tautomeric forms see ref *12*). The external aldimine has an absorption band only at 380 nm. The spectra of the two intermediates are essentially independent of the solution pH (Figure 1). This is consistent with the mechanism of eq 5, in which the PLP aldimine has a single protonation structure in both the Michaelis complex and the external aldimine. Decreasing the pH increases the amount of $EH^+{\cdot}SH^+$ and increases the fraction of the Michaelis complex (including both $EH^+{\cdot}S$ and $EH^+{\cdot}SH^+$) in the steady state. This can explain the pH-dependent shift in the steady-state spectra, that is, the decreasing of the 380-nm absorption band with decreasing pH (Figure 1).

DISCUSSION

The previous kinetic study at pH 7.0 showed that the association of AADC with dopa and further processing of the enzyme−substrate complexes can be followed in a stopped-flow spectrophotometer (*9*). The association rate constant for AADC and dopa was found to be of the order of 10^5 M^{-1} s^{-1} (*9*). This was a curious finding, because the enzyme−substrate association rate constants of many enzymes have been reported to be on the order of 10^7-10^8 M^{-1} s^{-1} (*13*). The present results showed that there are two routes for the association of AADC and dopa. The first is the association of the α-amino-group-unprotonated form of dopa and the enzyme to form a Michaelis complex (route A in Scheme 1) that directly undergoes transaldimination reaction to form the external aldimine complex. The second is the association of the α-amino-group-protonated form of dopa and the enzyme to form another Michaelis complex (route B in Scheme 1). This complex cannot directly undergo transaldimination and is converted to the first Michaelis complex by deprotonation (Scheme 1). The rate constants for the first and the second association processes were obtained to be 1.3×10^7 M^{-1} s^{-1} and 1.0×10^5 M^{-1} s^{-1}, respectively. The value for the first association process is a reasonable one for a bimolecular association reaction. It then became clear that the abnormally low value of the bimolecular association rate constant at pH 7.0 was due to the small fraction of the reactive form of the substrate at this pH. The active site of AADC is considered to be hydrophobic compared to other PLP enzymes, as indicated from the observation that the tautomeric equilibrium of the PLP-Lys303 aldimine is shifted toward the enolimine form, the prevalent species in apolar environments (*7*, *9*). The observation that the pK_a of the substrate α-amino group decreases by 2 pH units upon binding to AADC (compare K_a^{α} and $K_a^{\alpha M}$) and that the bimolecular association rate constant for the α-amino-group-protonated dopa is lower than that for the α-amino-group-unprotonated dopa by 2 orders of magnitude, are interpreted to be due to the unfavorable interaction of the protonated amino group with the hydrophobic active site.

The external aldimine complex, which is formed from $EH^+{\cdot}S$ by transaldimination, is expressed as a single species in eq 5. This has been supported by the pH-independent value of k_{-2}. However, this does not rule out the presence of more than one species that have an identical number of protons. In the external aldimine of the AspAT−2-methylaspartate complex, the proton shuttles between the imine N of the PLP-2-methylaspartate aldimine and the ϵ-amino group of Lys258 (the PLP-binding lysine in the unliganded enzyme), and therefore, the external aldimine is composed of two structures having different protonation states (*5*). We can consider a similar combination of structures for the external aldimine of AADC and dopa, as shown in Scheme 1. The absorption spectrum of the external aldimine is pH-independent and has a large absorption band with a λ_{max} of 380 nm (Figure 1). This absorption band is not that of typical protonated PLP aldimines, which have usually large absorption bands at 410−430 nm, but resembles that of unprotonated PLP aldimines, which have absorption bands at around 360 nm (*7*). Therefore, the absorption spectrum suggests that the external aldimine complex exists preferentially as the structure $H^+E{=}S$, the unprotonated aldimine form. The reason for the 20-nm red shift of the external aldimine of AADC from the ordinary unprotonated PLP aldimine is not clear at present. The unprotonated PLP aldimine has a tendency to adopt a conformation in which the imine bond is perpendicular to the pyridine ring (*5*). Accordingly, if we assume that the imine bond of the external aldimine of AADC resides in the plane of the pyridine ring through conformational constraints imposed by the active site, the π-overlap between the pyridine ring and the imine would increase, and this may account for the red shift of the absorption bands of the external aldimine.

In AspAT, $H^+E{=}S$ is catalytically inert, because the ϵ-amino group is the catalytic base that abstracts the proton from the substrate in the external aldimine (*1*). Therefore, AspAT is naturally designed to decrease the fraction of $H^+E{=}S$ in the external aldimine (*5*). In decarboxylases, however, the ϵ-amino group of the lysine residue is not necessary for decarboxylation of the external aldimine (*14*). This may allow the catalytic reaction to proceed from $H^+E{=}S$, the main species in the external aldimine of AADC. On the other hand, the absence of a proton on the imine N (or on O3′) decreases the electrophilicity of the coenzyme and can be an unfavorable factor for catalysis. Therefore, the driving force that promotes catalysis may be provided by the decarboxylation reaction itself, which is highly exergonic as compared to deprotonation.

The protonation of the quinonoid intermediate is another important issue. If we assume that the rate constant k_H corresponds to the step of protonation of the quinonoid intermediate, this intermediate would be accumulated at high pH. However, at pH 7.1, where k_H is 50 s^{-1} (compared to $k_{DC} = 8.0$ s^{-1}), no absorption was observed at around 500 nm (Figure 1). As the molar extinction coefficient for quinonoid intermediates at this wavelength is around 4×10^4 M^{-1} cm^{-1} (*7*), we should detect the species with high sensitivity. Even at pH 8.0, where k_H is expected to have a value of 6.2 s^{-1}, no apparent accumulation of the species

[3] As k_{+3} contains both k_{DC} and k_H, the absorption spectra of the external aldimine obtained at high pH values are considered to be mixtures of the external aldimines of PLP-dopa and PLP-dopamine. At pH 7.1, the PLP-dopamine is calculated to occupy 14% of the mixture ($k_{DC} = 8.0$ s^{-1} and $k_H[H^+] = 49$ s^{-1}). The complete absence of the absorption at around 425 nm (and no shoulder at around 335 nm) shows that the PLP-dopamine aldimine, like the PLP-dopa aldimine, exists as an unprotonated Schiff base. This is consistent with the mechanism shown in Scheme 1, in which the proton is transferred intramolecularly from O3′ of the quinonoid intermediate to Cα to form the PLP-dopamine aldimine unprotonated at the imine N.

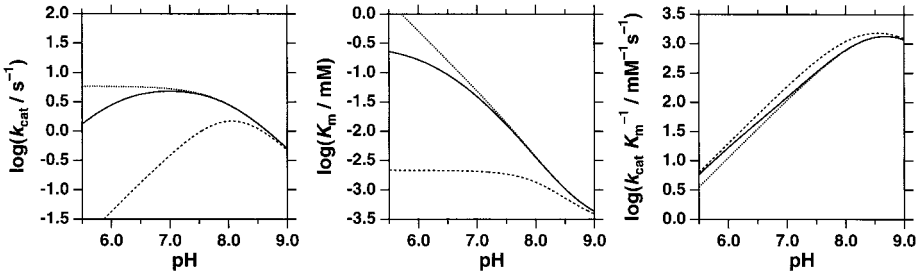

FIGURE 7: Simulation of the pH dependency of the steady-state kinetic parameters k_{cat}, K_m, and k_{cat}/K_m. Solid lines are those obtained by using eqs 8−11 and the microscopic kinetic parameters obtained in this study. Dotted lines are those from $k_{+1}^{SH} = 0$, and dashed lines are those from $k_{+1}^{SH} = 1.3 \times 10^7$ M^{-1} s^{-1}, while the other parameters are the same as those used to draw the solid lines.

was observed (data not shown). Therefore, we should consider that the quinonoid intermediate accepts a proton rapidly from a neighboring protonated base. To explain the rapid and stoichiometric disappearance of the quinonoid intermediate, this base must be fully protonated when the quinonoid intermediate is formed. The hydroxyl (O3′-H) group of the quinonoid intermediate can be a candidate for this protonated base. If this is the case, the ϵ-amino group of Lys303 may act as a catalyst for the proton transfer.[3] Then, k_H can be considered to correspond to the protonation of the external aldimine of PLP-dopamine (Scheme 1).

Contrary to the external aldimine, the Michaelis complex of AADC exchanges a proton with the solvent (eq 5 and Scheme 1). This is in contrast with the Michaelis complex of AspAT, which is composed of two structures with an identical number of protons (*4*). The Michaelis complex of AspAT has the closed conformation of the protein identical to that of the external aldimine complex. Due to this rigid structure, the substrate α-amino group and the PLP-Lys258 aldimine are in close proximity to each other, and the proton shuttles between the two bases, with no net exchange of protons with the solvent. It is, therefore, interesting to consider the conformational difference between the Michaelis complex and the external aldimine in AADC. AADC has a flexible region that is easily cleaved by proteases (*15*, *16*). This region can still be cleaved in the Michaelis complex but not in the external aldimine, indicating that the region retains its flexibility in the Michaelis complex and becomes rigid upon formation of the external aldimine (*16*). Taking the present observations together, we can consider that the flexibility of the enzyme protein of the Michaelis complex allows the solvent to access to the α-amino group of dopa. In other words, the α-amino group of the substrate and the imine N of the internal aldimine of the Michaelis complex are not as close in AADC as those in AspAT.

Is there physiological significance for the presence of the association of AADC and the substrate with a protonated α-amino group (route B in Scheme 1)? To address this question, we performed simulations of two extreme cases. The first is the case in which route B does not exist ($k_{+1}^{SH} = 0$), that is, AADC strictly binds the substrate with its α-amino group unprotonated. The second is the case in which route B has the same bimolecular association rate constant as route A ($k_{+1}^{SH} = 1.3 \times 10^7$ M^{-1} s^{-1}), that is, AADC does not distinguish the protonation state of the substrate α-amino group. In each case, the kinetic parameters other than k_{+1}^{SH} were fixed to the values shown in Scheme 1. The pH dependency of the steady-state kinetic parameters is shown in Figure 7. The overall tendency is that k_{cat} increases with increasing stringency of the enzyme that selectively accepts the substrate with an unprotonated α-amino group, and on the contrary, k_{cat}/K_m increases with decreasing stringency of the enzyme. The latter indicates that when the enzyme−substrate association becomes partially rate-determining in the overall catalytic reaction, such as when the substrate concentration is extremely low, binding of any substrate species to the enzyme, even if the species is unfavorable for subsequent catalysis, increases the catalytic efficiency. In fact, as the concentration of dopa within cells such as neurons in the striatum is considered to be of the order of millimolar (*17*), well above the K_m value at physiological pH, the evolutional constraint is imposed on the enzyme to increase k_{cat} and not k_{cat}/K_m. Accordingly, AADC has been evolved to carry out discrimination of the protonation state of the substrate α-amino group. However, at pH 7.4, decreasing the k_{+1}^{SH} value below 1.0×10^5 M^{-1} s^{-1} does not increase further the k_{cat} value (Figure 7). Therefore, it can be considered that the rate of evolution of AADC has slowed after k_{+1}^{SH} became as low as 1.0×10^5 M^{-1} s^{-1}.

In summary, the present study showed that the α-amino-group-unprotonated form of substrate preferentially binds to AADC, which has a protonated PLP-Lys303 aldimine. This is in contrast to the binding of aspartate to AspAT, in which a combination of the reverse protonation state of the PLP aldimine and the substrate is significant. AADC still allows the binding of the α-amino-group-protonated form of the substrate. This route merges to the main catalytic route by deprotonation of the α-amino group in the Michaelis complex. There seems to be no catalytic significance for the presence of this auxiliary route, and this seems to be the consequence of the minimum evolution of the enzyme sufficient for carrying out catalysis under physiological conditions.

REFERENCES

1. Kirsch, J. F., Eichele, G., Ford, G. C., Vincent, M. G., Jansonius, J. N., Gehring, H., and Christen, P. (1984) *J. Mol. Biol. 174*, 497−525.
2. Toney, M. D., and Kirsch, J. F. (1993) *Biochemistry 32*, 1471−1479.
3. Gloss, L. M., and Kirsch, J. F. (1995) *Biochemistry 34*, 3990−3998.
4. Hayashi, H., and Kagamiyama, H. (1997) *Biochemistry 36*, 13558−13569.
5. Hayashi, H., Mizuguchi, H., and Kagamiyama, H. (1998) *Biochemistry 37*, 15076−15085.
6. Ivanov, V. I., and Karpeisky, M. Y. (1969) *Adv. Enzymol. Relat. Areas Mol. Biol. 32*, 21−53.

7. Kallen, R. G., Korpela, T., Martell, A. E., Matsushima, Y., Metzler, C. M., Metzler, D. E., Morozov, Yu. V., Ralston, I. M., Savin, F. A., Torchinsky, Yu., M., and Ueno, H. (1985) in *Transaminases* (Christen, P., and Metzler, D. E., Eds.) pp 37−108, John Wiley & Sons, New York.
8. Ishii, S., Nishino, J., Mizuguchi, H., Hayashi, H., and Kagamiyama, H. (1996) *J. Biochem. (Tokyo) 120*, 369−376.
9. Hayashi, H., Mizuguchi, H., and Kagamiyama, H. (1993) *Biochemistry 32*, 812−818.
10. O'Leary, M. H., and Baughn, R. L. (1977) *J. Biol. Chem. 252*, 7168−7173.
11. Perrin, C. (1965) *Dissociation Constants of Organic Bases in Aqueous Solution*, p 394, Butterworths, London, U.K.
12. Zhou, X., and Toney, M. D. (1999) *Biochemistry 38*, 311−320.
13. Fersht, A. (1985) *Enzyme Structure and Mechanism*, 2nd ed., pp 150−151, Freeman, New York.
14. Nishino, J., Hayashi, H., Ishii, S., and Kagamiyama, H. (1997) *J. Biochem. (Tokyo) 121*, 604−611.
15. Tancini, B., Dominici, P., Simmaco, M., Schinina, M. E., Barra, D., and Voltattorni, C. B. (1988) *Arch. Biochem. Biophys. 260*, 569−576.
16. Ishii, S., Hayashi, H., Okamoto, A., and Kagamiyama, H. (1998) *Protein Sci. 7*, 1802−1810.
17. Vellan, E. J., Gjessing, L. R., and Stalsberg. H. (1970) *J. Neurochem. 17*, 699−701.
18. Momany, C., Ghosh, R., and Hackert, M. L. (1995) *Protein Sci. 4*, 849−854.
19. Momany, C., Ernst, S., Ghosh, R., Chang, N. L., and Hackert, M. L. (1995) *J. Mol. Biol. 252*, 643−655.

BI9909795